

## **DECOMPOSITION OF IRON-BASED MARTENSITE A kinetic analysis by means of differential scanning calorimetry and dilatometry**

*P. V. Morra<sup>1</sup>, A. J. Böttger<sup>2</sup> and E. J. Mittemeijer<sup>3</sup>*

<sup>1</sup>Netherlands Institute for Metals Research, Rotterdamseweg 137, 2628 AL Delft, The Netherlands

<sup>2</sup>Delft University of Technology, Laboratory of Materials Science, Rotterdamseweg 137,  
2628 AL Delft, The Netherlands

<sup>3</sup>Max Planck Institute for Metals Research, Seestrasse 92, D-70174 Stuttgart, Germany

### **Abstract**

The decomposition processes of a carburised Fe–C alloy, a Fe–C, a Fe–Cr–C and commercial SAE 52100 cast alloys (with a C content of about 1 mass%) have been studied by means of differential scanning calorimetry and dilatometry. The combination of these two experimental techniques is very powerful and allows the identification of all the stages occurring during tempering. Activation energies have been obtained by performing a Kissinger-like analysis and were used to infer the rate-determining step for each stage of decomposition. This parallel investigation allowed to determine the effect of the alloying elements on the different stages of tempering.

**Keywords:** iron-based martensite, kinetic, precipitation, tempering

### **Introduction**

Iron-based martensites ( $\alpha'$ ) are supersaturated solid solutions of interstitial carbon (nitrogen) atoms in a metal lattice [1] obtained by quenching from the austenitic phase field. The obtained martensitic material is hard and brittle and is used in tool parts only after heat treatment. The material properties are optimised by adding alloying elements to the iron matrix and by choosing the appropriate tempering treatment. In particular for high precision parts as bearing components like rings and rollers the heat treatment is crucial to prevent dimensional changes of the parts in use caused by phase transformations [2].

The microstructure of the as-quenched martensitic commercial steels consists of three different phases: martensite, retained austenite ( $\gamma_R$ ) and carbides (only present in the as-cast materials) that remained partly undissolved after the austenitisation treatment and the quench performed in order to obtain the martensitic structure. The tempering process of these alloys can be divided in six different stages [3, 4], occurring at different temperature ranges, which can vary depending on the steel composition and microstructure:

(i), (ii) The first two stages, referred to as the 'preprecipitation processes' and occurring below 353 K, consist of the segregation of carbon atoms to lattice defects and the formation of clusters of carbon atoms in the iron matrix.

(iii) The third stage, associated with the precipitation of a transition carbide (first discovered by Jack [5] and referred to as  $\epsilon$  carbide and later as  $\eta$  carbide by Nagakura [6]), occurs in the temperature range of about 353–453 K.

(iv) The fourth stage, taking place in the temperature range of about 473–623 K is associated with the transformation of retained austenite into ferrite ( $\alpha$ ) and cementite ( $\theta$ , an orthorhombic  $M_3C$  carbide) and has been found to occur in two successive steps [4]: the transformation of austenite into ferrite and carbon-enriched austenite, starting already during the last part of the third stage of tempering and the decomposition of the carbon-enriched austenite into ferrite and cementite.

(v) The fifth stage, occurring at temperatures of about 523–773 K, involves the conversion of the transition carbide into cementite.

(vi) The sixth stage, assigned to the dissolution of cementite particles and the formation of more stable alloy carbides occurs only if strong carbide formers as chromium, molybdenum, tungsten, vanadium are present and takes place at temperatures of about 723–973 K.

In this paper the tempering processes of martensites obtained from cast material Fe–C, Fe–Cr–C, SAE 52100 and by carburising pure Fe, are reported. The effect of alloying elements (Cr in particular) on the decomposition behaviour of these interstitial  $\alpha'$  is investigated in the temperature range from room temperature (RT) to 823 K by using differential scanning calorimetry (DSC) and dilatometry. The use of these two complementary experimental techniques is essential in this investigation because some of the phase transformations (segregation and clustering of carbon atoms) show a significant heat release but almost no length change whereas others (precipitation of cementite) are attended with a pronounced length change and a small heat release. This combined calorimetric and dilatometric analysis allows the identification and kinetic analysis of all the stages occurring upon tempering.

Activation energies have been obtained by performing a Kissinger-like analysis [7] and were used to infer the rate-determining step for each stage of decomposition.

## Experimental procedures

### *Specimens preparation*

Four different materials (a carburised and three cast alloys) have been investigated. The compositions of the cast alloys have been given in Table 1. After casting alloys A and B have been processed in hot iso-static press at a temperature of 1423 K and a pressure of 120 MPa during 2 h, followed by slow cooling, allowing some homogenisation and the elimination of any porosity. Finally a soft annealing treatment, consisting of austenitising at 1093 K for 1 h followed by a slow cooling ( $10 \text{ K h}^{-1}$ ) to 963 K and by an air cooling, was performed.

**Table 1** Compositions of the cast alloys investigated in the present work (mass%)

	Cr	C	Mn	Si	Ni	Cu	Mo	Al	S	P
Alloy A	0.02	0.97	0.09	0.01	0.03	0.007	0.009	0.005	0.008	0.006
Alloy B	1.39	0.98	0.09	0.01	0.03	0.008	< 0.01	0.008	0.008	0.006
Alloy SAE 52100	1.36	1.01	0.32	0.25	0.16	0.12	0.04	0.034	0.020	0.013

Small discs with diameter of about 5 mm and thickness of about 0.2–0.3 mm have been cut from the cast pieces to be used for the DSC and XRD experiments. These discs have been austenitised in a vertical tube furnace at 1133 K for 14 min under a H<sub>2</sub> flow and then quenched in order to obtain the martensitic structure. A first set of specimens has been quenched in brine (10 mass% NaCl in water) at room temperature (BQ) and a second set of specimens has been quenched in brine at room temperature and subsequently in liquid nitrogen (BQ+LNQ).

The samples have been protected against decarburisation during the austenitising treatment by using Condursal 0090 paint. For the preparation of martensitic specimens for the dilatometer experiments see section Dilatometry.

For the preparation of the pure Fe–C alloys by carburising, pure 0.005 C, 0.0003 N, 0.01 mass% O, (Cr+Al+Mo+Cu+W) < 0.04 mass%, balance Fe) discs with diameter of about 5 mm and thickness of about 0.2 mm were used. The specimens were slightly etched in nital 2% for 5 min before carburizing, in order to remove the oxide layer on the surface. The carburizing was performed in a vertical tube furnace at a temperature of 1173 K in a gas stream consisting of a mixture of H<sub>2</sub> and CO. After carburizing the specimens were quenched in brine at RT (BQ); some of them were subsequently quenched in liquid nitrogen (BQ+LNQ). The carbon contents (0.93±0.05 mass%) have been determined by weighing the specimens before and after carburising.

### *Kinetic analysis*

The values of activation energy for the phase transformation occurring during tempering of the martensitic alloys have been determined using a Kissinger-like method [7] based on the equation:

$$\ln \frac{T_f^2}{\phi} = \frac{E}{RT_f} + \text{constant} \quad (1)$$

where  $R$  is the gas constant,  $T_f$  is the transformation temperature corresponding to a certain fraction ( $f'$ ) of phase transformed and  $\phi$  is the heating rate in K min<sup>-1</sup>. The peak maximum has been chosen in most of the cases as  $T_f$ ; when it was not possible to distinguish a distinct peak maximum (DSC measurements pertaining to the segregation of carbon atoms for all the alloys and to the formation of cementite for the carburised alloy) because of the overlap with another phase transformation,  $T_f$  was cho-

sen as the point where the slope of the measured curve (i.e. the measured heat flow) diverges 2% from the tangent of the rising part of the peak [4].

#### Differential scanning calorimetry

Differential scanning calorimetry was performed using a Perkin Elmer DSC7 apparatus in a protective atmosphere of Ar. Calibration was performed by measuring the well-established melting points of high purity indium and lead. The mass of the specimens used varied between 30 and 60 mg. After being weighed, each sample was sealed in an aluminium sample pan under an atmosphere of Ar (95%) and H<sub>2</sub> (5%) to avoid oxidation. An empty pan was used as a reference. Specimens were heated from 303 to 773 K with heating rates ( $\phi$ ) of 5 to 30 K min<sup>-1</sup> in case of the cast alloys and of 5 to 20 K min<sup>-1</sup> in case of the carburised alloys and then cooled down to 303 K; the baseline was determined by reheating the specimens with the same heating rates.

The values of activation energy for the first three stages of tempering of the martensitic alloys A, B, SAE 52100 and the carburised Fe–C (BQ) and the first four stages of tempering of martensitic alloy A and carburised Fe–C alloy (BQ+LNQ) have been determined on the basis of the transformation temperature data taking into account the thermal lag and the response time of the DSC.

#### Dilatometry

Dilatometry was carried out using a Bähr dilatometer type 805. Specimens of alloys B (length=5 mm, diameter=5 mm) and SAE 52100 (length=7 mm, diameter=4 mm) have been heated up to 1133 K in 5 min, kept at that temperature for 14 min under vacuum (10<sup>-4</sup> mbar), quenched to 303 K in He (denoted by QM, i.e. quench mode) and then tempered up to 823 K with heating rates of 5 to 20 K min<sup>-1</sup>. Specimens of alloy A (length=5mm, diameter=4 mm) have been heated up to 1133 K in 5 min, kept at that temperature for 14 min under vacuum (10<sup>-4</sup> mbar), quenched to 183 K in He (denoted by DC, i.e. deep cooling mode) in order to reach a quenching rate high enough to allow the formation of martensite. Then the specimens were tempered up to 823 K with heating rates of 5 to 20 K min<sup>-1</sup>. In order to determine the transformation temperatures pertaining to each phase transformation the data have been arithmetically averaged over time and subsequently differentiated with respect to the temperature. The values of activation energy for the precipitation of  $\epsilon/\eta$  carbide, the decomposition of  $\gamma_R$  and the formation of cementite of the martensitic alloys B and SAE 52100 and for the precipitation of  $\epsilon/\eta$  carbide and the formation of cementite of alloy A (the activation energy pertaining to the decomposition of retained austenite could not be determined because quenching the samples to 183 K leads to a martensitic structure with almost no retained austenite) have been determined using this technique.

## Results and discussion

The heat evolutions and changes in specific length induced in the investigated alloys by non-isothermal annealing employing a heating rate of 10 K min<sup>-1</sup> are shown in

**Table 2** Activation energy values for tempering processes in Fe–C based martensites derived from non-isothermal-annealing experiments (kJ mol<sup>-1</sup>)

	DSC alloy A BQ/BQ+LNQ	DSC alloy B BQ/BQ+LNQ	DSC alloy SAE 52100 BQ/BQ+LNQ	DSC carburised Fe-0.93±0.05 mass% C BQ/BQ+LNQ	Dilatometry alloy A DC	Dilatometry alloy B QM	Dilatometry alloy SAE 52100 QM
Segregation and clustering of C atoms	_/81	_/89	_/94	_/82	–	–	–
Precipitation of ε/η transition carbide	118/106	114/103	111/105	142/129	135	115	120
Decomposition of retained austenite (γ <sub>R</sub> )	135/138	141/141	144/145	141/141	–	156	150
Precipitation of cementite (θ)	_/198	–	–	_/212	195	164	163

Figs 1 and 2. The amounts of heat and length change observed depend on the relative volume fraction of the phases present in the as-quenched martensitic specimens and will not be discussed here.

#### *Segregation and clustering of carbon atoms*

Segregation and clustering [4], do not show a distinct length change, but are characterised by a significant heat release (Fig. 1). The heat effect due to these transformations overlaps with the heat effect of the subsequent transformation (the precipitation of the  $\epsilon/\eta$  transition carbide) and therefore it is not possible to discern a distinct peak

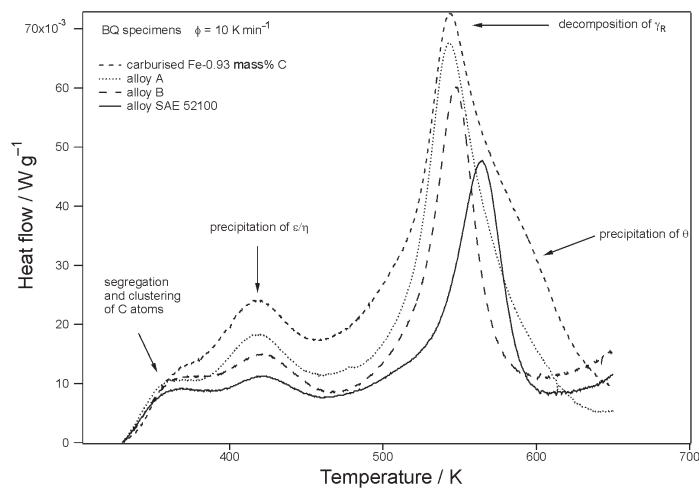


**Fig. 1** DSC curves of four martensitic specimens on isochronal annealing

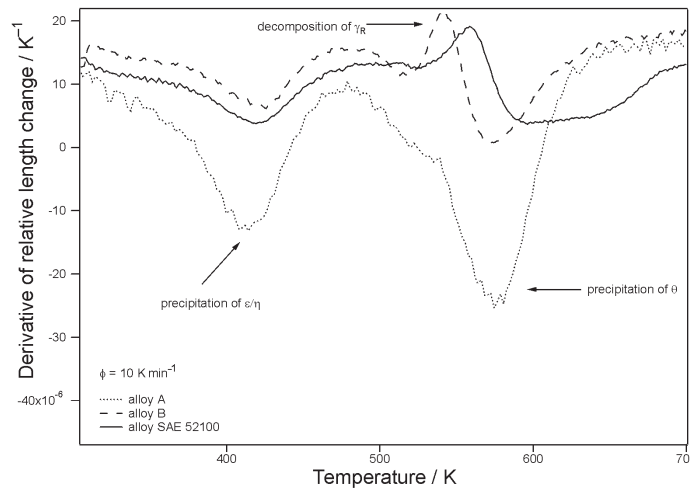


**Fig. 2** Derivative of relative length change on isochronal annealing of three martensitic specimens

maximum. The activation energy was determined as indicated in section Kinetic analysis. According to the high resolution transmission electron microscopy results [8] the segregation of carbon atoms to dislocations and grain boundaries is followed by the development of carbon enrichments of variable carbon content that become a modulated, periodic structure as the decomposition goes on. This modulated structure disappears after tempering above 373 K.

The activation energy values for these transformations determined for the BQ+LNQ specimens are in the range 81–94 kJ mol<sup>-1</sup>, in good agreement with the values found in literature [9] for Fe–C martensite. The diffusion of carbon in martensite is considered as the rate-determining step for the preprecipitation stages.

#### *Precipitation of the $\epsilon/\eta$ transition carbide*

The transformation corresponding to the second peak of Fig. 1 (differential scanning calorimetry) and to the first peak of Fig. 2 (dilatometry) occurs for all the alloys in the temperature range 353–453 K. It has been associated [4] with the precipitation of a transition carbide and it shows both pronounced heat production and significant length decrease.

The activation energies found for this process for the cast alloys are somewhat higher for the BQ samples than for the BQ+LNQ samples (Table 2). Except for alloy B the dilatometer experiments result in somewhat higher values for the activation energy; a quantitative comparison is hampered by the differences in quenching procedure for the specimens used for DSC and dilatometry. The activation energies obtained agree well with the value of the activation energy found in literature [10] (113 kJ mol<sup>-1</sup>, obtained from dilatometer experiments [11] for five high purity Fe–C alloys and two commercial steels varying in carbon content from 0.6 to 1.4 mass%).

The values obtained for the carburised alloy are somewhat higher than the ones obtained for the cast alloys. The activation energies are in between those for diffusion of C in  $\alpha$ -Fe and those for diffusion of iron along dislocations (i.e. pipe diffusion, 152 kJ mol<sup>-1</sup> [12]). Dislocations are expected to occur upon  $\epsilon/\eta$  precipitation in order to accommodate the specific volume misfit between the transition carbide and the matrix. It is suggested that the observed effective activation energy is the result of nucleation and growth processes of the transition carbide (Appendix 2 in Ref. [7]). For the cast alloys the kinetics is expected to be dominated by growth of the carbides and volume diffusion of interstitial atoms in martensite because the carbides (undissolved during austenitisation) already present in the as-quenched martensite, serve as nucleation sites.

On the basis of resistivity measurements the effect of carbide forming alloying elements on the precipitation of the transition carbide is reported to reduce the activation energy of the order of 5 to 10 kJ mol<sup>-1</sup> per mass% alloying element [13]. In the present investigation no influence of the alloying elements could be observed within the accuracy of the activation energy data ( $\pm 5$  kJ mol<sup>-1</sup>).

The transformation temperature for the precipitation of the transition carbide is the same for the carburised and the pure cast Fe–C alloys and is somewhat higher for

the Cr-containing alloys B and SAE 52100. This suggests that chromium is the element that retards the precipitation of the transition carbide.

#### *Decomposition of retained austenite*

The decomposition of retained austenite [4], occurring in the temperature range of about 473–623 K, causes a large heat production and a pronounced length increase. The decomposition of retained austenite and the formation of cementite (length decrease) overlap completely (Fig. 1). The activation energy values obtained for the decomposition of retained austenite are in the range 135–156 kJ mol<sup>-1</sup>, agreeing well (in particular the DSC data) with the values of the activation energy calculated on the basis of [14] and [15] for the carbon content dependent diffusion of carbon in austenite, suggesting carbon diffusion in austenite as the rate-determining step for the phase transformation. Because of the presence of undissolved carbides the carbon content of retained austenite will be lower than the nominal carbon content. The carbon contents of the retained austenite and martensite of the cast alloys have been determined by means of X-ray diffraction using the dependence on the carbon content of the lattice parameters [16]. The results are shown, together with the calculated activation energy values, in Table 3. The values determined for alloys B and SAE 52100 are higher than that in the case of alloy A but the increase in activation energy is not as pronounced as expected on the basis of the extrapolation of carbon diffusion data [17] (i.e. ~30 kJ mol<sup>-1</sup> in Fe–0.8 mass% C–1.41 mass% Cr) which could be caused by the presence of undissolved carbides which are expected to contain a significant part of the Cr. Alternatively, the data could also be interpreted as pertaining to interface controlled growth, according with the kinetic analysis (140 kJ mol<sup>-1</sup>) for the  $\gamma \rightarrow \alpha$  transformation in Fe–Mn alloys [18]. Then the activation energy for this stage of tempering is expected to be independent of the carbon content.

**Table 3** Carbon contents of the martensitic matrix of the cast alloys and corresponding activation energy values [14]

	C/mass%	C/at%	Activation energy for diffusion of C in $\gamma$ /kJ mol <sup>-1</sup>
Alloy A carburised Fe–0.93 mass% C	0.93	4.16	138
Alloy B	0.73	3.26	140
Alloy SAE 52100	0.70	3.12	141

The shift towards higher temperatures of the phase transformation (occurring at 541, 546 and 563 K respectively for alloys A, B and SAE 52100,  $\phi=10$  K min<sup>-1</sup>) is ascribed to the effect of alloying elements on the diffusion of carbon in austenite because these alloys contain respectively 0, 1.36 and 1.82 mass% austenite stabilising [19] elements (such as manganese, nickel and chromium).



### *Precipitation of cementite*

This phase transformation, occurring upon tempering between about 523 and 723 K [4] is associated with a small change of enthalpy and with a significant length decrease and therefore only dilatometry could be applied to investigate the kinetics of this stage of tempering. It was possible to use differential scanning calorimetry only in the case of the carburised alloy and alloy A BQ+LNQ, where the overlap between the fourth and the fifth stages of tempering is just partial and the peak pertaining to the decomposition of retained austenite is smaller than in the case of the BQ samples. Clearly, the alloying elements play an important role in this transformation (Fig. 2): the temperature range of the transformation shifts towards higher temperatures for the alloys in the order: alloy A, alloy B, alloy SAE 52100. Also the shape of the length change depends on the alloy composition. In the case of alloy A the derivative of the length change with respect to the temperature is rather symmetrical, in the case of alloy B it is somewhat asymmetric and for what concerns alloy SAE 52100 a strong asymmetry is observed. According to the data reported in literature [20] for a medium carbon steel, chromium (but also nickel and manganese) shift the temperature of the end of the process towards higher temperatures while other alloying elements such as silicon, even in small concentration, tend to increase the transformation temperatures.

The values of activation energy determined are in the range 163–212 kJ mol<sup>-1</sup>, in between the values indicated in literature for the pipe diffusion of iron [12] (152 kJ mol<sup>-1</sup>) and the volume diffusion of iron [21] (251 kJ mol<sup>-1</sup>). Therefore, the activation energy obtained could be interpreted as an effective one combining these two mechanisms. Note that the pipe diffusion of iron atoms, that may occur along dislocations that form to accommodate the volume misfit caused by the phase transformation, may be less dominant for the precipitation of cementite than in the case of the precipitation of the transition carbide. The precipitation of cementite occurs in fact at higher temperatures, where the volume diffusion becomes relatively more important.

\* \* \*

The authors are grateful to J. Slycke, M. Persson and P. Neuman of the SKF Engineering Research Centre for provision of the cast materials and their advice about the dilatometry experiments. Thanks are also expressed to Ing. N. M. van der Pers for his help with the X-ray diffraction experiments.

### **References**

- 1 C. M. Wayman, Introduction to the Crystallography of Martensitic Transformations, Macmillan 1964.
- 2 E. B. Mikus, T. J. Hughel, J. M. Gerty and A. C. Knudsen, Trans. ASM, 52 (1960) 307.
- 3 G. R. Speich, Metals Handbook, Vol. 8, ASM, 1973, p. 202.
- 4 M. J. van Genderen, A. Böttger, Th. H. de Keijser and E. J. Mittemeijer, Metall. Trans. A, 28A (1997) 545.
- 5 G. Krauss, Principles of Heat Treatment of Steels, American Society for Metals, Metals Park, Ohio 44073, 1980.

- 6 S. Nagakura, Y. Hirotsu, M. Kusunoki, T. Suzuki and Y. Nakamura, *Metall. Trans. A*, 14A (1983) 1025.
- 7 E. J. Mittemeijer, *J. Mat. Science*, 27 (1992) 3977.
- 8 K. Han, M. J. van Genderen, A. Böttger, H. W. Zandbergen and E. J. Mittemeijer, *Phil. Mag. A*, 8A (2000) 311.
- 9 L. Cheng, C. M. Brakman, B. M. Korevaar and E. J. Mittemeijer, *Metall. Trans. A*, 19A (1988) 2415.
- 10 B. S. Lement and M. Cohen, *Acta Met.*, 4 (1956) 469.
- 11 C. S. Roberts, B. L. Averbach and M. Cohen, *Trans. ASM*, 45 (1953) 576.
- 12 M. Cohen, *Trans. JIM*, 11 (1970) 145.
- 13 H.W. King and S. G. Glover, *JISI*, 196 (1960) 281.
- 14 J. Ågren, *Scripta Met.*, 20 (1986) 1507.
- 15 C. Wells, W. Batz and R. F. Mehl, *Trans. AIME*, 188 (1950) 553.
- 16 L. Cheng, A. Böttger, Th. H. de Keijser and E. J. Mittemeijer, *Scripta Met. et Mat.*, 24 (1990) 509.
- 17 M. Munirajulu, B. K. Dhindaw and A. Biswas, *Scripta Mat.*, 37 (1997) 1693.
- 18 G.P Krielaart and S. van der Zwaag, *Mat. Sci. and Techn.*, 1998 (14) 10.
- 19 E. C. Bain and H. W. Paxton, *Alloying Elements in Steel*, American Society for Metals, 1966, p. 124.
- 20 A. S. Kenneford and T. Williams, *JISI*, 185 (1957) 467.
- 21 F. S. Buffington, K. Hirano and M. Cohen, *Acta Met.*, 9 (1961) 434.